

COMPARISON OF THE FLOW IN CO-ROTATING AND COUNTER-ROTATING TWIN-SCREW EXTRUDERS

A. Shah and M. Gupta

*Mechanical Engineering-Engineering Mechanics Department
Michigan Technological University, Houghton, MI 49931*

Abstract

Polymeric flow in intermeshing co-rotating and counter-rotating twin-screw extruders is simulated. Effect of the elongational viscosity of the polymer on the flow in the two extruders is included by using independent Carreau models for the shear and elongational viscosities of the polymer. It is found that for similar screw cross-sections and rotational speed, axial velocity as well as degree of mixing is higher in the co-rotating extruder, whereas pressure build up is higher in the counter-rotating extruder. In contrast to the flow in the co-rotating extruder, where the velocity was always maximum at the screw tips, in the counter rotating extruder the velocity was higher in the intermeshing zone.

Introduction

Co-rotating and counter-rotating twin-screw [1 – 3] extruders are commonly used in plastic industry for applications ranging from melting and pumping of polymer for profile extrusion to compounding, mixing, devolatilization and chemical reaction. Besides the drag-induced flow in the translational region, which is the sole mode of polymer transport in single screw extruders, the positive displacement characteristics in the intermeshing region makes twin-screw extruders particularly suitable for processing hard-to-feed materials and thermally sensitive materials such as PVC, which may require short and narrowly distributed residence time. Since the counter-rotating twin-screw extruders, which are similar to gear pumps, provide the maximum positive displacement, they are the machine of choice for profile extrusion, whereas co-rotating twin-screw extruders are more suitable for other applications such as compounding, mixing, devolatilization and chemical reaction. The main reason for suitability of twin-screw extruders for these applications is the complexity of the flow in the intermeshing region, which provides them good mixing and compounding characteristics. However, the complexities of the flow makes it difficult to predict the performance of a twin-screw extruder and also difficult to design an extruder given the performance requirements. Consequently, simple design equations, which are commonly available for single-screw extruders, are difficult to obtain for twin-screw extruders. Because of this complexity and lack of predictability, the screws for

twin-screw extruders are typically available as interchangeable elements. By exploring various feasible combinations, this modular design allows appropriate selection of the screw elements according to the required flow characteristics. Such a trial-and-error approach not only consumes valuable time, but rarely provides an optimal design for a specific application.

A three-dimensional simulation of the flow can be exploited as an excellent aide for design of twin-screw extruders. Because of the lack of reliable and easy-to-use software packages for three-dimensional simulation of polymeric flows, in the past, modular design of screw elements and exploration of various combinations of these elements, was probably the best option available to a twin-screw extruder designer. However, with the development of efficient flow simulation packages and tremendous growth in computational power, full three-dimensional simulation of the flow in the twin-screw extruders is now feasible [4 – 15]. In particular, in reference [14], we analyzed the effects of elongational viscosity on the flow in a twin-screw extruder. Based upon the flow simulations with the same shear viscosity but different elongational viscosities, it was concluded that the axial component of velocity, that is, the throughput of a co-rotating twin-screw extruder, is smaller, whereas the pressure build-up is higher for higher elongational viscosity. In the present work, the flow in a co-rotating twin-screw extruder is compared with the flow in a geometrically similar counter-rotating twin-screw extruder. The PELDOM software [16] is used in simulating the flow in the two extruders. Besides capturing the shear-thinning behavior of polymeric viscosity, this software also accounts for the strain-rate dependence of elongational viscosity of the polymer. The geometry of the twin-screw extruder, and the shear and elongational viscosity models used in the present work are discussed next.

Geometry of the Twin-Screw Extruders

The dimensions of the co-rotating twin-screw extruder used here (Table 1) are the same as those used in reference [14]. As shown in Fig. 1 (b), a counter-rotating twin-screw extruder with the same screw cross-sections as those used for the co-rotating extruder was used for the purpose of flow comparison. In particular, the cross-sectional dimensions of the kneading discs used by

Ishikawa et al. [7], were used to obtain the two twin-screw extruders used in present work. The screw cross-sections were rotated in the same and in the opposite directions to obtain the co-rotating (Fig 1 a) and counter-rotating (Fig 1 b) twin-screw extruders, respectively. For both the extruders, the two-lobe cross-section was rotated through 540° with the screw lead of 30 mm to obtain 45 mm axial lengths of the screws. For the flow simulations reported later in the paper, the two co-rotating screws in Fig. 1 (a) were rotated in the clockwise direction at 60 RPM, whereas the left and right counter-rotating screws in Fig 1 (b) were rotated in the clockwise and counter-clockwise directions, respectively.

Shear and Elongational Viscosity Models

In the present work, the Carreau model was used for the shear as well as the elongational viscosities of the polymer. However, the software allows completely independent parameters for the shear and the elongational viscosity models.

$$\eta_s = \eta_o (1 + (\lambda e_{II})^2)^{(n-1)/2}$$

$$\eta_a = 3\eta_o (1 + (\lambda_a e_{II})^2)^{(m_a-1)/2}$$

$$\eta_p = 4\eta_o (1 + (\lambda_p e_{II})^2)^{(m_p-1)/2}$$

where η_s is the shear viscosity, η_a and η_p are the axisymmetric and planar elongational viscosities, η_o is the zero-shear viscosity, λ , λ_a , λ_p , m , m_a , m_p are material parameters, e_{II} , the second invariant of the strain-rate tensor, is the same as the shear rate tensor for shear viscosity and is $\sqrt{3}\dot{\epsilon}$ for a axisymmetric elongational viscosity and $2\dot{\epsilon}$ for planar viscosity. The values of the various material parameters used for the flow simulation in this work are as follows.

$$n = 0.4, \quad \lambda = \lambda_a = \lambda_p = 536 \text{ s}$$

$$\eta_o = 124,000 \text{ Pa.s}, \quad m_a = m_p = 0.6$$

Results and Discussion

The finite element meshes used to simulate the flow in the co-rotating and counter-rotating twin-screw extruders are shown in Figs. 2 (a) and (b) respectively. The co-rotating extruder mesh in Fig. 2 (a) has 313,830 elements, whereas the counter-rotating extruder mesh in Fig. 2 (b) has 303,334 elements. The software uses linear tetrahedral finite element elements, which allows the mesh generation over such complex domains as the flow domain in twin-screw extruders. If brick-type elements are used, the finite element mesh generation in such a domain will be extremely difficult and time consuming. The circumferential velocity corresponding to the angular velocity of 60 RPM was specified on the nodes of the screw surfaces. As mentioned before, both the screws in the co-rotating extruder were rotated in the clockwise direction, whereas in the counter-rotating extruder, left

screw was rotated in the clockwise direction and the right screw was rotated in the counter-clockwise direction. The no-slip condition was enforced on the barrel surfaces, whereas the no-traction condition was employed at the entrance and exit of the two extruders.

The velocity distributions in two of the cross-sections of the co-rotating and counter-rotating extruders are shown in Fig. 3. In Figs. 3 – 5, the upper and lower cross-sections are, respectively, 10 and 40 mm away from the entrance, with the total length of the extruder being 45 mm. The arrows in Fig. 3 show the direction of velocity, whereas the color of the arrows depicts the magnitude of the velocity. The velocity distributions in the co-rotating (Fig. 3 a) and counter-rotating (Fig. 3 b) extruders have very different characteristics. In the co-rotating extruder the maximum velocity is always at the tips of the two screws. On the other hand, in the intermeshing region of the counter-rotating extruder, since the velocity on the surface of both screws is in the same direction, the polymer has a strong tendency to move in the cross-sectional plane. Consequently, the maximum velocity in the counter-rotating extruder is in the intermeshing region. Another important distinction in the velocity distributions in Figs. 3 (a) and (b) is that in each rotation of the co-rotating extruder, most of the fluid in one lobe is transferred to the other lobe, which is not necessarily true for the counter-rotating extruder. Therefore, in comparison to counter-rotating extruders, co-rotating extruders are expected to provide better mixing of polymers, which explains their popularity for applications such as compounding, devolatilization and chemical reactions.

Fig. 4 shows the variation in the axial component of velocity in the co-rotating and counter-rotating extruders. The magnitude of the axial velocity in the co-rotating extruder (Fig. 4 a) is significantly higher than that in the counter-rotating extruder (Fig. 4 b). Therefore, if the extruder has no die in front or a die with a relatively small pressure drop across it, a co-rotating extruder is expected to provide higher throughput than a similar counter-rotating extruder. However as discussed in the next paragraph, this may not be true if the die in front of the twin-screw extruder provides a strong restriction to the flow. In the co-rotating extruder, the maximum axial velocity is in the intermeshing region, whereas the intermeshing region of the counter-rotating extruder, where the traverse velocity is very high, the axial velocity is actually negative, that is, the flow is in the reverse direction. In the counter-rotating extruder the maximum axial velocity is typically in some position away from the intermeshing region.

Fig. 5 shows the pressure distribution in two of the cross sections of the co-rotating and counter-rotating extruders. The predicted pressure on the barrel and screw surfaces of the two extruders is shown in Fig. 6. Since the pressure in Figs. 5 and 6 has a very large range and the

extreme values are reached, only in a small region near the screw flights, to accurately show the pressure away from the screw flights, a logarithm scale has been used for the coloring scheme in Figs. 5 and 6. It should be noted that in Figs. 5 and 6 the variation in pressure, and not the actual value of pressure, is important, because the actual values of the pressure will change depending upon which die is installed in front of the extruder. In Figs. 5 and 6, in co-rotating as well as counter-rotating extruder, there is a sharp pressure drop across screw flights, with the pressure being very high in front of the leading edge and very low behind the trailing edge of the flight. Since the screws in the co-rotating extruder are rotated in the clockwise direction, the left screw pushes the polymer in upper intermeshing zone, which is taken away by the right screw. Therefore in the upper half of the co-rotating extruder, the pressure is high in the left lobe and low in the right lobe. The opposite is true in the lower half of the co-rotating extruder, because the motion is reversed in the lower half. In contrast, in the counter rotating extruder, since the right side screw is rotating in counter-clockwise direction, both the screws push the polymer in the upper intermeshing region and take the polymer away from the lower intermeshing region. Therefore, in the counter rotating extruder, the pressure is high in the complete upper half of the extruder and low in the lower half. It is also noted that the maximum pressure build-up in the counter-rotating extruder (Figs. 5 b, 6 b) is higher than that in the counter rotating extruder (Figs. 5 a, 6 a). Because of this larger pressure and the corresponding larger throughput, counter-rotating extruders are preferred for pumping the molten polymer in profile extrusion.

Conclusions

Flow of a polymer, employing independent shear and elongational viscosity models, was simulated in co-rotating and counter-rotating twin-screw extruders. In the co-rotating extruder the maximum velocity was obtained at the screw tips, whereas the maximum velocity in the counter-rotating extruder was in the intermeshing region. Since, in each rotation of a co-rotating extruder, the polymer in one lobe is transferred to the other lobe, it was argued that co-rotating extruders provide better mixing than the counter-rotating extruders. However, the counter-

rotating twin-screw extruder was found to generate a greater pressure build-up and therefore should be preferred over co-rotating extruders for profile extrusion.

References

1. J. L. White, *Twin Screw Extrusion*, Hanser Publishers, New York (1992).
2. C. Rauwendaal, *Polymer Extrusion*, Hanser Publishers, New York (1994).
3. D. G. Baird and D. I. Collias, *Polymer Processing*, John Wiley and Sons, Inc. (1998).
4. A. Kiani, J. E. Curry and P. G. Anderson, *SPE ANTEC Tech. Papers*, **44**, 48 (1998).
5. A. Lawal, S. Railkar and D. M. Kalyon, *SPE ANTEC Tech. Papers*, **45**, 317 (1999).
6. T. Avalosse, Y. Rubin, *SPE ANTEC Tech. Papers*, **45**, 322 (1999).
7. T. Ishikawa, S. Kihara and K. Funatsu, *Polym. Eng. Sci.*, **40**, 357 (2000).
8. V. L. Bravo, A. N. Hrymak, J. D. Wright, *Polym. Eng. Sci.*, **40**, 525 (2000).
9. B. Alsteens, V. Legat, T. Avalosse and T. Marchal, *SPE ANTEC Tech. Papers*, **48**, 194 (2002).
10. X. Ma, X. Geng and L. Zhu, *SPE ANTEC Tech. Papers*, **49**, 142 (2003).
11. L. Zhu, K.A. Narh and K. S. Hyan, *SPE ANTEC Tech. Papers*, **49**, 147 (2003).
12. X. Ma, Y. Yin, X. Geng and L. Zhu, *SPE ANTEC Tech. Papers*, **49**, 152 (2003).
13. B. Alsteens, T. Avalosse, V. Legat, T. Marchal and E. Slachmuylders, *SPE ANTEC Tech. Papers*, **49**, 173 (2003).
14. A. Shah and M. Gupta, *SPE ANTEC Tech. Papers*, **49**, 322 (2003).
15. O. Wunsch, Ralf Kuhn and P. Heidemeyer, *SPE ANTEC Tech. Papers*, **49**, 338 (2003).
16. PELDOM software, Plastic Flow, LLC, 1206 Birch Street, Houghton, MI 49931.

Key Words: Twin-screw extrusion, Elongational viscosity, Finite element method.

Table 1: Dimensions of the twin-screw extruder.

	(mm)
Barrel Diameter	30.0
Screw tip diameter	29.2
Screw root diameter	21.0
Centerline distance	26.0
Screw lead	30.0

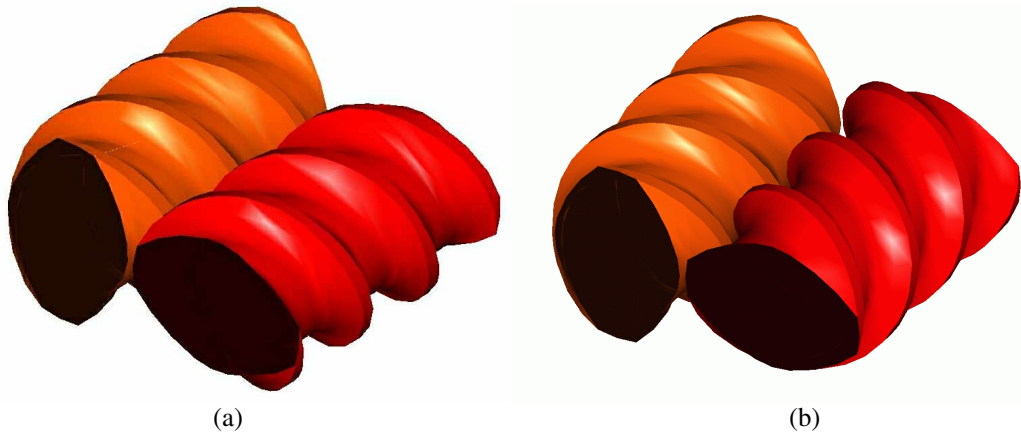


Fig.1. Geometry of the intermeshing screws in co-rotating (a) and counter-rotating (b) twin screw extruders.

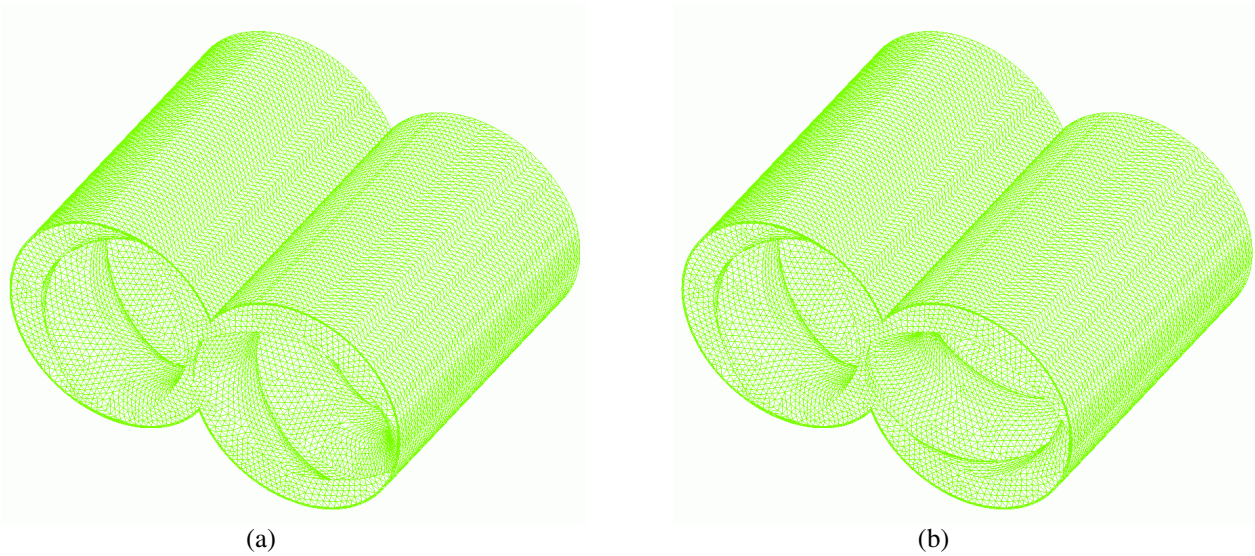


Fig 2. Finite element meshes used for flow simulation in co-rotating (a) and counter-rotating (b) twin-screw extruders.

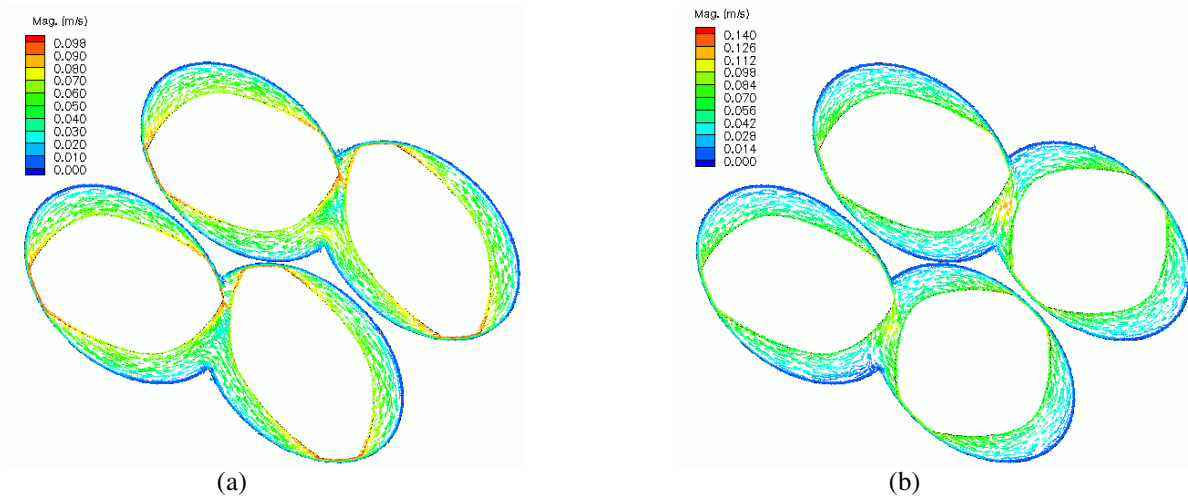


Fig 3. Velocity distribution in two of the planes perpendicular to the axis of the co-rotating (a) and counter-rotating (b) twin-screw extruders.

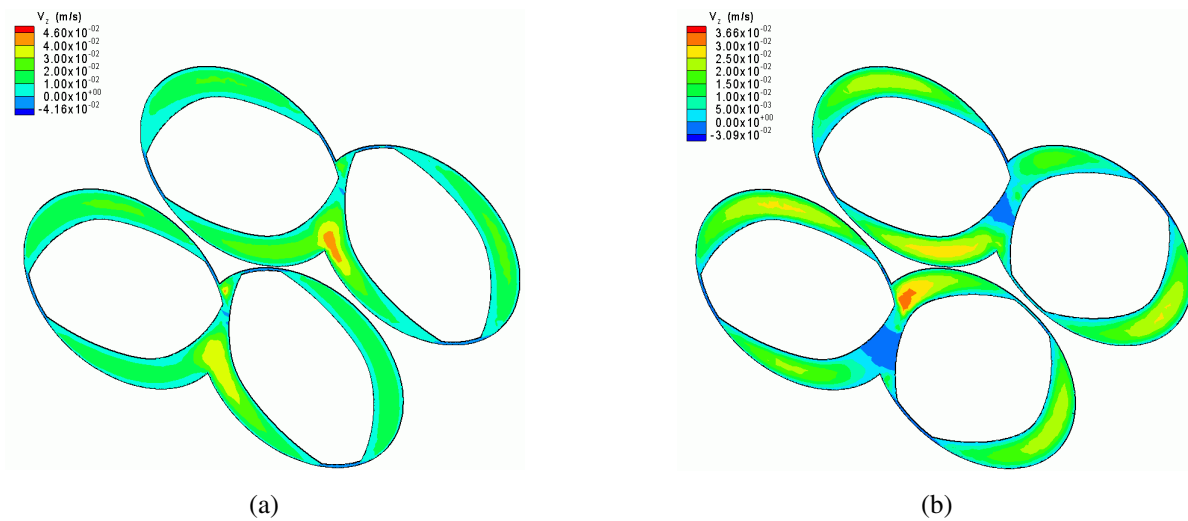


Fig 4. Axial velocity distribution in two of the planes perpendicular to the axis of the co-rotating (a) and counter-rotating (b) twin-screw extruders.

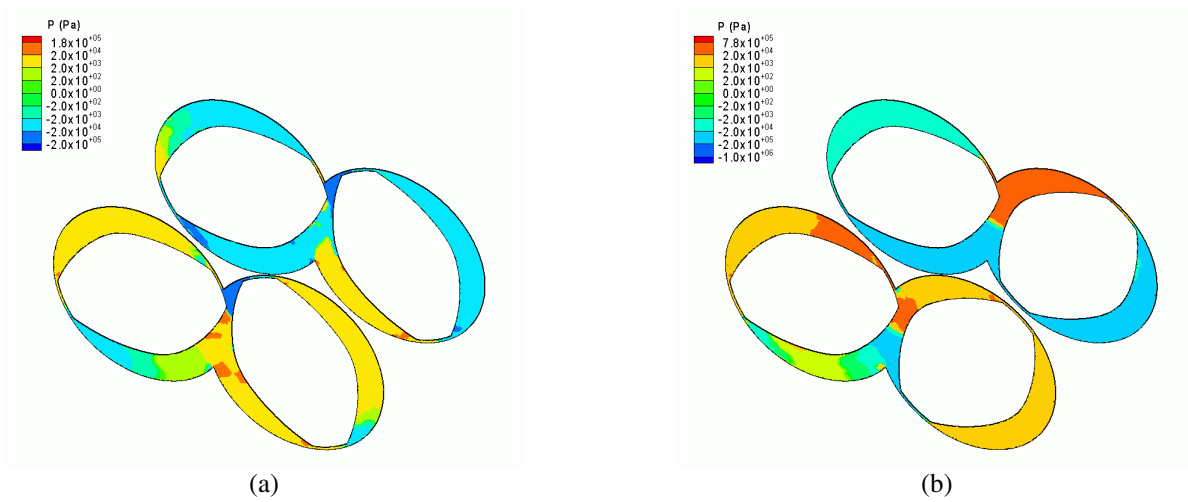


Fig 5. Pressure distribution in two of the planes perpendicular to the axis of the co-rotating (a) and counter-rotating (b) twin-screw extruders.

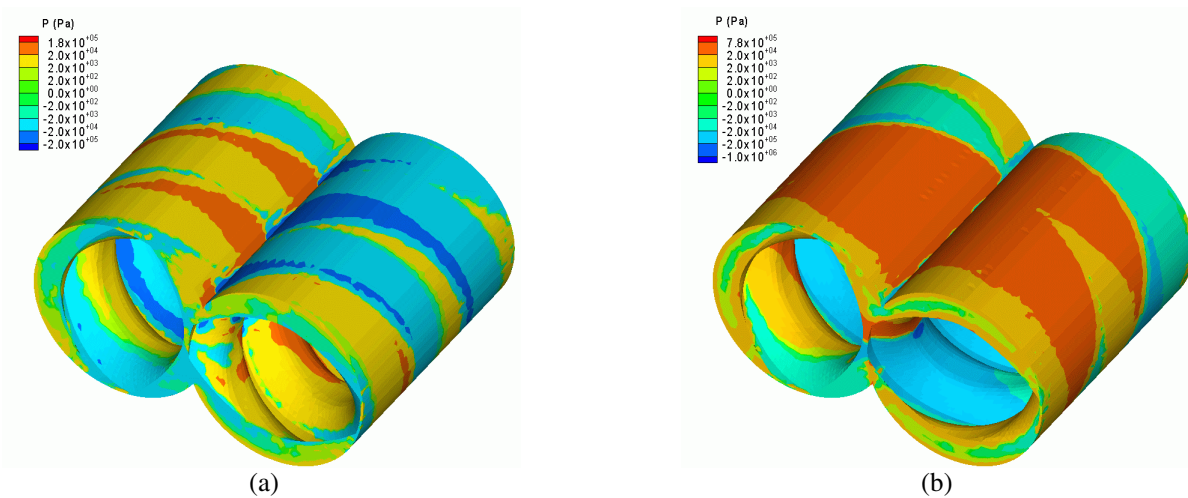


Fig 6. Pressure distribution on the barrel surfaces of the co-rotating (a) and counter-rotating (b) twin-screw extruders.